Interaction of cecropin A analogs with DNA analyzed by multi-spectroscopic methods

Libo Yuan (lbyuan@haut.edu.cn)
Henan University of Technology
Ke Wang
Henan University of Technology
Yuan Fang
Zhengzhou People's Hospital
Xiujuan Xu
Henan University of Technology
Yingcun Chen
Henan University of Technology
Dongxin Zhao
Henan University of Technology
Kui Lu
Henan University of Technology

Research Article

Keywords: cecropin A, analogs, cationic amino acids, antimicrobial peptides, spectroscopic methods

Posted Date: September 22nd, 2023

DOI: https://doi.org/10.21203/rs.3.rs-3357236/v1

Abstract

Cecropin A is a cationic antimicrobial peptides which contain lots of basic amino acids. To understand the effect of basic amino acids on cecropin A, analogues CA2, CA3 and CA4 which have more arginine or lysine at the N-terminal or C-terminal were designed and synthesized. The interaction of cecropin A and its analogs with DNA was studied using ultraviolet-visible spectroscopy, fluorescence spectroscopy and circular dichroism spectroscopy. Multispectral analysis showed that basic amino acids improved the interaction between the analogues and DNA. The interaction between CA4 and DNA is most pronounced. Fluorescence spectrum indicated that Ksv value of CA4 is 1.19×10^5 L·mol^{-1} compared to original peptide cecropin A of 3.73×10^4 L·mol^{-1}. The results of antimicrobial experiments with cecropin A and its analogues showed that basic amino acids enhanced the antimicrobial effect of the analogues. The antimicrobial activity of CA4 against *E. coli* was 8-fold higher than that of cecropin A. The importance of basic amino acid in peptides is revealed and provides useful information for subsequent studies of antimicrobial peptides.

Introduction

Bacterial infections have received more and more attention in recent decades. In 2019, these bacterial pathogens caused 7.7 million deaths worldwide, accounting for 13.6% of all global deaths (Murray et al. 2022). Antibiotics are very effective in preventing and treating bacterial infections. However, with the misuse of antibiotics, some bacteria have developed resistance (Bombaywala et al. 2021; Larsson and Flach 2022), and even multidrug-resistant bacteria have emerged (Nohl et al. 2020). Unfortunately, the development of conventional antibiotics has not kept pace with the rate at which bacteria are developing resistance. More than 100 antibiotics were discovered between 1920 and 1980, but few new antibiotics have been discovered in the last 40 years (Ulery 2016). There is an urgent need to find a safe and efficient alternative that is less prone to drug resistance.

Antimicrobial peptides (AMPs) are widely recognized as potential alternatives to antibiotics (Ali et al. 2022; Wang et al. 2019a). They are widely found in animals, plants and microorganisms and are an important part of the innate immune system (Magana et al. 2020; Yang et al. 2020). AMPs have broad-spectrum activity against a wide range of bacteria, viruses, fungi, parasites and even cancer cells (Luong et al. 2020). They also have chemotaxis, apoptosis, immunomodulation and wound healing effects (Zhong et al. 2017). AMPs are not susceptible to drug resistance due to their special bactericidal mode (Zhang et al. 2020). In addition, AMPs have many advantages, such as high specificity, good thermal stability, high antimicrobial activity and low mammalian cytotoxicity (Datta and Roy 2021). Therefore, AMPs hold great promise as a safe and effective new antibacterial drug (Spänig and Heider 2019). Cecropin A, a cationic antimicrobial peptide which has an alpha-helical structure with the core sequence KWKLFKK, was selected for this research. It has antibacterial, antiviral and anti-inflammatory biological activities and does not affect the eukaryotic cells (Wang et al. 2019b). To understand the effect of basic amino acids on cecropin A, analogues which have more arginine or lysine at the N-terminal or C-terminal were designed and synthesized. Structural simulation was used to investigate the structure change with the addition of arginine or lysine on cecropin A. The interaction of cecropin A and its analogs with DNA was studied using ultraviolet-visible, fluorescence and circular dichroism spectroscopy techniques. Finally, the antibacterial activity of the synthesized antimicrobial peptides was tested.

Materials and methods

Materials

Acetic anhydride, N, N-Dimethylformamide (DMF), tert-Butyl menthyl ether, methanol were purchased from Kemiou (Tianjin, China) Chemical Reagent Co. 2-(7-Azabenzotriazol-1-yl)-N, N, N', N'-tetramethyluronium hexafuorophosphate (HATU), 1-hydroxybenzotriazole (HOBT), trifuoro acetic acid (TFA), thioanisole were purchased from Macklin (Shanghai, China) Biochemical Technology Co. Fmoc-Wang Resin and amino acids were purchased from GL Biochem (Shanghai, China) Ltd. Phenol were purchased from Wind Ship (Tianjin, China) Chemical Reagent Technology Co. Ct-DNA was purchased from Sigma (Shanghai, China) Co. Ltd. *S.enteritidis* (CICC 21482), *S.aureus* (ATCC 25923), *L. monocytogenes* (ATCC 19115) and *E.coli* (ATCC 25922) were obtained from Zhengzhou People's Hospital. Ninhydrin hydrate, N, N-diisopropylethylamine (DIEA), 2-mercaptoethanol purchased from Aladdin (Shanghai, China) Biochemistry Technology Co.

Synthesis of Peptide

All peptides were synthesized from the C-terminus to the N-terminus according to the peptide sequence by using solid phase synthesis method. The typical synthesis steps are as follows: Weigh 1.0 g of Fmoc-Wang Resin into a 100 mL solid phase peptide synthesis tube, 15 mL of DMF was added and stirred with nitrogen for 40 mins. DMF was filtered and then 15 mL of 20% piperidine solution was added to the synthesis tube with nitrogen puffing for 15 mins to remove the protecting Fmoc group. After deprotection, the resin was washed sequentially with DMF, anhydrous methanol, DMF, anhydrous methanol, DMF. Afterward, the exact amino acids and activators (HATU, HOBT, DIEA) were weighed and completely solubilized using DMF. The prepared coupling solution was poured into the synthesis tube and reacted for 2 hrs under light-proof conditions. The washing, deprotection and coupling steps were repeated until peptide synthesis was complete. Both deprotection and coupling results were tested using ninhydrin hydrate. After sealing the peptide ends, 15 mL of cutting agent was prepared for cutting. The volume ratio of the cutting agent was 82.5% TFA, 5% thioanisole, 5% 2-mercaptoethanol, 5% water and 2.5% phenol. After cutting was completed, the solution was suction filtered into tert-butyl methyl ether and frozen overnight. Finally, the peptide was obtained by centrifugation.

Mass Spectrometry (MS) Characterization

The mass spectra of synthesized peptides were determined using an LCQ Fleet Mass Spectrometer (Thermo Fisher Scientific, USA) in positive ion mode with an ESI ion source. The peptide solution concentration was 1 mg/mL and was dissolved using deionized water.

Peptide Structural and Bioinformatics Analysis

Peptide sequences were primarily analyzed by ProtParam (https://web.expasy.org/protparam/). The likelihood that the synthetized peptide is AMPs was analyzed using the AMP Predictor (APD3 Server, https://aps.unmc.edu/) and CAMPR3 server (http://www.camp.bicnirrh.res.in/). The three-dimensional structures of peptides were predicted by I-TASSER online server (https://zhanggroup.org/I-TASSER/) (Yang et al. 2022).

Ultraviolet-visible (UV) Spectrum characterization

UV spectroscopy was carried out using a Cary 60 (Agilent Technologies, USA). Dispense 3 mL of ct-DNA solution (C_{ct-DNA}=50 μM, pH = 7.4, 5×Tris-HCl buffer) into a cuvette and add 3 μL of peptide solution ($C_{peptide}$=1×10^{-3} M) to the cuvette drop at a time. At the same time, 3 μL of peptide solution ($C_{peptide}$=1×10^{-3} M) was added dropwise to 3

mL of 5×Tris-HCl buffer solution as a reference solution. After mixing and standing for 10 mins, the UV spectrum of the ct-DNA were recorded at 230–350 nm.

Fluorescence Spectrum Characterization

Fluorescence spectroscopy was performed using Fluoromax Plus (HORIBA, Japan). The excitation wavelength is 525nm, the test wavelength range is 530-750nm and the slit width is 5nm. Dispense 3 mL of DNA-EB solution (C_{ct-DNA}=50 μM, C_{EB}=5 μM) into a cuvette and add 3 μL of peptide solution ($C_{peptide}$=1×10^{-3} M) to the cuvette drop at a time. After mixing and standing for 10 mins, the fluorescence spectra of the DNA-EB system were measured.

Circular Dichroic (CD) Spectrum Characterization

CD detection was performed using a J-1500 CD spectrophotometer (JASCO, Japan). A short-stranded DNA solution with a concentration of 10 μM was prepared and the peptide solution was added. A DNA-peptide solution with a peptide solution concentration of 40 μM was finally obtained. After mixing and standing for 10 mins, the CD spectra was measured. The scanning wavelength range was 220–320 nm with a gap width of 0.5 nm.

Antimicrobial activity test

The the minimum inhibitory concentration (MIC) values of the samples against the strains were determined using standard micro broth dilution method. Bacteria were cultured using fresh LB broth and diluted to 1×10^{5} CFU·mL^{-1} when used. Add 100μL of peptide sample to the first column of the 96-well plate and dilute to the 10th column by double dilution method. Columns 11 and 12 serve as controls. Finally 100μL of bacterial solution was added to each well. After incubation at 37 ℃ for 20 hrs, the transmittance of the bacterial solution was measured using a microplate reader to determine MIC of the peptide.

Results and Discussion

Design and Synthesis of Peptides

Cationic AMPs are rich in basic amino acids such as arginine, histidine and lysine. These basic amino acids give AMPs an overall positive net charge at physiological pH. The amount of positive charge can influence the electrostatic adsorption of AMPs to negatively charged phospholipids in cell membranes and their antibacterial effect (Gagnon et al. 2017). Therefore, cecropin A analogs with more arginine or lysine at the N-terminal or C-terminal were designed. Table 1 lists the sequences and related data for cecropin A and its analogs. CA2 adds three arginines to the C-terminus of CA, CA3 adds three lysines to the N-terminus of CA, and CA4 adds three arginines to the C-terminus and three lysines to the N-terminus of CA. Figure 1 shows predicted three-dimensional structures of CA and its analogues. All three analogs showed an increase in hydrophilicity, positive charge number and a-helix structure compared to CA. All synthesized peptides were characterized by MS (Fig S1-S4).

Table 1
Characterization results and related data for synthetic peptides.

Peptide	Sequence	PI	Net charge	GRAVY	Theoretical MW	Measured MW		Discriminant Analysis
						$[M + 2H]^{2+}$	$[M + 3H]^{3+}$	
CA	KWKLFKK	10.48	+ 4	-1.414	1019.28	510.33	—	0.914
CA2	KWKLFKKRRR	12.31	+ 7	-2.340	1487.83	744.58	496.83	0.971
CA3	RRRKWKLFKK	12.31	+ 7	-2.340	1487.83	744.58	496.83	0.981
CA4	KKKKWKLFKKRRR	12.32	+ 10	-2.700	1872.35	937.17	625.08	0.997

The grand average of hydropathicity (GRAVY) is computed by the hydrophilic values of all amino acids. Measured MW was measured using ESI-MS. The higher value of AMP discriminant analysis

means the greater possibility of being an antimicrobial peptide.

Ultraviolet-visib le Spectrum Analysis

UV spectroscopy is an effective tool for studying peptide-DNA interactions. DNA has chromophores such as aromatic bases and phosphate groups, which have strong absorption peaks around 260 nm in the UV absorption spectrum. When a peptide interacts with DNA, the binding mode of the peptide to the DNA based on the hyperchromic/hypochromic effect of the characteristic DNA absorption peaks and the red/blue shift of the characteristic absorption peaks can be determine[d] (Sirajuddin et al. 2013; Jaumot and Gargallo 2012). There are three types of binding modes for peptides to DNA: groove binding mode, electrostatic binding mode and intercalation binding mode. The electrostatic binding mode occurs between the positively charged polypeptide and the phosphate backbone of the DNA. It will contract the steric helix of the DNA double helix structure, resulting in a hypochromic effect (Zhao et al. 2015). The groove binding mode is where bases in DNA interact with small molecules. It causes a change in the structure of the DNA double helix, resulting in a hyperchromic effect (Zhou et al. 2015). The intercalation binding mode is where small polypeptide molecules are embedded in the hydrophobic region of DNA base pairs and bound to DNA by π-π stacking and hydrophobic interactions. A significant red shift and hypochromic effect usually occurs as a result of typical intercalation binding mode (Charak et al. 2011).

As shown in Fig. 2, with increasing concentrations of CA and its analogs, the maximum absorption peak at 260 nm for ct-DNA showed a hyperchromic effect and was accompanied by a slight red shift. This suggests that the mode of interaction of the CA peptide and its analogs with ct-DNA is not a typical intercalation binding mode, but possibly an electrostatic or groove binding mode. The analogs CA2, CA3 and CA4 contain more arginine or lysine than CA. The side chains of these amino acids carry guanidine and amino groups that can reach into the internal grooves of the DNA helix and act on the bases of the DNA, exposing the base pairs and causing an increase in the UV absorption of the DNA. Thus, the interaction of CA2, CA3 and CA4 with ct-DNA results in a more pronounced hyperchromic effect than CA.

Fluorescence Spectrum Analysis

Ethidium bromide (EB) is commonly used as a fluorescent probe in the study of DNA-small molecule interactions (McKeever et al. 2013). The fluorescence of both DNA and EB itself is very weak. However, when EB is inserted between base pairs within the DNA double helix, the fluorescence intensity of the DNA-EB system is greatly enhanced (Chen et al. 2000). As shown in Fig. 3, the DNA-EB system underwent fluorescence quenching as the peptide concentration in the DNA-EB system increased.

The fluorescence quenching can be described by the Stern-Volmer equation:

$$\frac{F_0}{F} = 1 + K_{SV}[Q] = 1 + K_q \tau_0 [Q]$$

Ksv is the Stern-Volmer quenching constant, K_q is the quenching rate constant, F_0 is the fluorescence intensity of the DNA-EB system in the absence of the peptide solution, F is the fluorescence intensity of the DNA-EB-peptide system, [Q] is the peptide solution concentration, and τ_0 is the lifetime of the fluorophore without the peptide solution. The fluorescence lifetime of a large biomolecule is approximately 10^{-8}s (Lakowicz and Weber 1973). Figure 4 is obtained by plotting F_0/F against [Q]. The binding constants of CA, CA2, CA3 and CA4 to DNA calculated from the slopes of the fitted lines are shown in Table 2.

Table 2
Stern-Volmer quenching constants KSV and quenching rate constants Kq for the interaction of peptides with DNA-EB systems.

Peptide	K_{SV} ($L \cdot mol^{-1}$)	K_q ($L \cdot mol^{-1} \cdot s^{-1}$)	R
CA	3.73×10^4	3.73×10^{12}	0.9631
CA2	5.83×10^4	5.83×10^{12}	0.9695
CA3	1.1×10^5	1.1×10^{13}	0.9982
CA4	1.19×10^5	1.19×10^{13}	0.9755

The binding constant of EB to ct-DNA is 2.6×10^6 $L \cdot mol^{-1}$ (Bi et al. 2008), which is much higher than that of CA ($3.73\times10^4 L \cdot mol^{-1}$), CA2 ($5.83\times10^4 L \cdot mol^{-1}$), CA3 ($1.1\times10^5 L \cdot mol^{-1}$) and CA4 ($1.19\times10^5$ $L \cdot mol^{-1}$). Therefore, it is difficult for CA and its analogs to replace EB and bind to ct-DNA by insertion. The mode of binding of CA and its analogues to ct-DNA is presumed to be a mixture of groove binding and electrostatic binding, rather than an intercalation binding mode based on fluorescence spectrum. Both electrostatic binding mode and groove binding mode cause fluorescence quenching in the ct-DNA-EB system. Positively charged amino acid residues can electrostatically bind to the negatively charged phosphate backbone of ct-DNA, causing the ct-DNA double strand to tighten and extrude the EB. The guanidine and amino groups on their side chains can also reach into the grooves of ct-DNA and break the hydrogen bonding forces between ct-DNA base pairs, exposing the base pairs of ct-DNA and causing EB release (Sarwar et al. 2015). The analogs CA2, CA3 and CA4 contain more more arginine or lysine. Therefore, they all have a larger K_{SV} than CA and the change in fluorescence quenching is more pronounced. It can be inferred that the more basic amino acids in a peptide the greater its ability to bind to ct-DNA.

Fluorescent quenching can be categorized into dynamic quenching and static quenching. The collision of fluorescent molecules in the excited state with the quencher molecule can lead to dynamic fluorescence quenching. Static quenching is caused by the creation of non-fluorescent material molecules when the quencher molecules are in the ground state with the fluorescent molecules. The collision constant for the maximum diffusion control of fluorescent molecules by small molecules is 2×10^{10} $L\cdot mol^{-1}\cdot s^{-1}$ (Abdelhameed et al. 2019). The Kq of CA and its analogs is greater than 2×10^{10} $L\cdot mol^{-1}\cdot s^{-1}$. Thus the quenching effect of CA and its analogues on DNA-EB is static quenching.

Circular Dichroism Analysis

Guanine-rich DNA or RNA sequences self-assemble by G-tetrad π π stacking to form a special nucleic acid secondary structure, the G-quadruplex structure (Burge et al. 2006). The different structures of the G-quadruplex correspond to different absorption peaks. The CD spectrum has a negative characteristic absorption peak at 240 nm and a positive characteristic absorption peak at 260 nm, indicating a parallel structure. The CD spectrum has a negative characteristic absorption peak at 260 nm and a positive characteristic absorption peak at 290 nm, indicating a antiparallel structure. The CD spectrum has a positive characteristic absorption peak at 235–240 nm, indicating a hybrid structur (Kypr et al. 2009).

Figure 5 shows that CA acts with Guanine-rich DNA G1 and G2 can form parallel G-quadruplex structures. The sequences of short-stranded DNA G1 and G2 were agggagggcgggaggagggg and agggtggggagggtgggg. The reduced CD signal after incubation with analogs CA2, CA3 and CA4 suggests that the stacking between the G-tetrad bases is disrupted. The presumed reason for this is that CA2, CA3 and CA4 have more positively charged amino acids that bind more strongly to the sequence DNA. This is consistent with the phenomenon of the unfolding of the fourfold structure.

Antibacterial activity

The MIC values of the samples were determined for strains *S.enteritidis*, *E.coli*, *S.aureus* and *L.monocytogenes*. As shown in Table 3, the analogs CA2, CA3 and CA4 showed more antimicrobial activity than CA. The reason for this is hypothesized to be that the analogs CA2, CA3 and CA4 have more positive charges and more obvious a-helix structures that interact effectively with DNA. The best antimicrobial activity was CA4, which showed an 8-fold higher antimicrobial activity against *E. coli* compared to CA. These antibacterial results are consistent with previous spectroscopic results.

Table 3
Antibacterial activity of the ligands

Peptide	MIC(μM)			
	S. enteritidis	*E. coli*	*S. aureus*	*L. monocytogenes*
CA	32	16	> 256	32
CA2	16	16	128	8
CA3	8	8	128	8
CA4	8	2	64	8

Conclusion

In this work, a cationic antimicrobial peptides CA and three analogues were designed and synthesized and characterized by MS. Multispectral results indicate that peptides with more basic amino acid interact more strongly with DNA. Fluorescence spectrum indicated that Ksv value of CA4 is 1.19×10^5 $L\cdot mol^{-1}$ compared to original peptide CA of 3.73×10^4 $L\cdot mol^{-1}$. Our studies show that the synthesized peptides can bind ct-DNA in a groove-bound form, accompanied by electrostatic interactions. The results of antibacterial tests show that the inhibitory activity of the analogs CA4 was significantly enhanced compared to CA. This can be attributed to having a more positive charges and a more pronounced a-helix structures carried on CA4. The antimicrobial activity of CA4 against *E. coli* was 8-fold higher than that of CA. The above results reveal the importance of basic amino acid in AMPs and provide new ideas for the study of novel antimicrobial peptides.

Declarations

Acknowledgements:

This work was supported by the National Natural Science Foundation of China [grant number 21708005, 21572046], Science and Technology Foundation of Henan Province [grant number 222102310545], Cultivation Programme for Young Backbone Teachers in Henan University of Technology [grant number 21420111] and National Pharmaceutical Care Foundation of China Medicine Education Association [grant number CMEAPC2023016]. We thank Figdraw (www.figdraw.com) for expert assistance in the graphical abstract drawing.

Conflict of interest:

The authors declare that they have no conflict of interest.

Authors contribution

Libo Yuan: Supervision, Methodology, Writing—review and editing. **Ke Wang**: Methodology, Writing—original draft preparation. **Yuan Fang**: Supervision, Antimicrobial experiments. **Xiujuan Xu**: Peptides synthesis. **Yingcun Chen**: Peptides synthesis. **Dongxin Zhao**: Spectral data analysis. **Kui Lu**: Supervision, Writing—review and editing.

References

1. Abdelhameed AS, Bakheit AH, AlRabiah HK, Hassan ES, Almutairi FM (2019) Molecular interactions of AL3818 (anlotinib) to human serum albumin as revealed by spectroscopic and molecular docking studies. J Mol Liq 273:259–265. https://doi.org/10.1016/j.molliq.2018.10.025
2. Ali W, Elsahn A, Ting DSJ, Dua HS, Mohammed I (2022) Host defence peptides: a potent alternative to combat antimicrobial resistance in the era of the covid-19 pandemic. Antibiot (Basel Switzerland) 11(4). https://doi.org/10.3390/antibiotics11040475
3. Bi S, Zhang H, Qiao C, Sun Y, Liu C (2008) Studies of interaction of emodin and DNA in the presence of ethidium bromide by spectroscopic method. Spectrochim Acta Part A Mol Biomol Spectrosc 69(1):123–129. https://doi.org/10.1016/j.saa.2007.03.017

4. Bombaywala S, Mandpe A, Paliya S, Kumar S (2021) Antibiotic resistance in the environment: a critical insight on its occurrence, fate, and eco-toxicity. Environ Sci Pollut Res 28(20):24889–24916. https://doi.org/10.1007/s11356-021-13143-x
5. Burge S, Parkinson GN, Hazel P, Todd AK, Neidle S (2006) Quadruplex DNA: sequence, topology and structure. Nucleic Acids Res 34(19):5402–5415. https://doi.org/10.1093/nar/gkl655
6. Charak S, Jangir DK, Tyagi G, Mehrotra R (2011) Interaction studies of Epirubicin with DNA using spectroscopic techniques. J Mol Struct 1000(1–3):150–154. https://doi.org/10.1016/j.molstruc.2011.06.013
7. Chen W, Turro NJ, Tomalia DA (2000) Using ethidium bromide to probe the interactions between DNA and dendrimers. Langmuir 16(1):15–19. https://doi.org/10.1021/la981429v
8. Datta S, Roy A (2021) Antimicrobial peptides as potential therapeutic agents: a review. Int J Pept Res Ther 27:555–577. https://doi.org/10.1007/S10989-020-10110-X
9. Gagnon MC, Strandberg E, Grau-Campistany A et al (2017) Influence of the length and charge on the activity of α-helical amphipathic antimicrobial peptides. Biochemistry 56(11):1680–1695. https://doi.org/10.1021/acs.biochem.6b01071
10. Jaumot J, Gargallo R (2012) Experimental methods for studying the interactions between G-quadruplex structures and ligands. Curr Pharm Design 18(14):1900–1916. https://doi.org/10.2174/138161212799958486
11. Kypr J, Kejnovská I, Renčiuk D, Vorlíčková M (2009) Circular dichroism and conformational polymorphism of DNA. Nucleic Acids Res 37(6):1713–1725. https://doi.org/10.1093/nar/gkp026
12. Lakowicz JR, Weber G (1973) Quenching of fluorescence by oxygen. Probe for structural fluctuations in macromolecules. Biochemistry 12(21):4161–4170. https://doi.org/10.1021/bi00745a020
13. Larsson DJ, Flach CF (2022) Antibiotic resistance in the environment. Nat Rev Microbiol 20(5):257–269. https://doi.org/10.1038/s41579-021-00649-x
14. Luong HX, Thanh TT, Tran TH (2020) Antimicrobial peptides–Advances in development of therapeutic applications. Life Sci 260:118407. https://doi.org/10.1016/j.lfs.2020.118407
15. Magana M, Pushpanathan M, Santos AL (2020) The value of antimicrobial peptides in the age of resistance. Lancet Infect Dis 20(9):e216–e230. https://doi.org/10.1016/S1473-3099(20)30327-3
16. McKeever C, Kaiser M, Rozas I (2013) Aminoalkyl derivatives of guanidine diaromatic minor groove binders with antiprotozoal activity. J Med Chem 56(3):700–711. https://doi.org/10.1021/jm301614w
17. Murray CJL, Ikuta KS, Sharara F et al (2022) Global burden of bacterial antimicrobial resistance in 2019: a systematic analysis. The Lancet 10325:399. https://doi.org/10.1016/S0140-6736(21)02724-0
18. Nohl A, Hamsen U, Jensen KO et al (2020) Incidence, impact and risk factors for multidrug-resistant organisms (MDRO) in patients with major trauma: a European Multicenter Cohort Study. Eur J Trauma Emerg Surg 1–7. https://doi.org/10.1007/s00068-020-01545-4
19. Sarwar T, Rehman SU, Husain MA, Ishqi HM, Tabish M (2015) Interaction of coumarin with calf thymus DNA: deciphering the mode of binding by in vitro studies. Int J Biol Macromol 73:9–16. https://doi.org/10.1016/j.ijbiomac.2014.10.017
20. Sirajuddin M, Ali S, Badshah A (2013) Drug–DNA interactions and their study by UV–Visible, fluorescence spectroscopies and cyclic voltametry. J Photochem Photobiol B 124:1–19. https://doi.org/10.1016/j.jphotobiol.2013.03.013

21. Spänig S, Heider D (2019) Encodings and models for antimicrobial peptide classification for multi-resistant pathogens. BioData Min 12(1):1–29. https://doi.org/10.1186/s13040-019-0196-x
22. Ulery BD (2016) SNAPPy solution for fighting drug-resistant bacteria. Sci Transl Med 8(360). 360ec164-360ec164
23. Wang J, Song J, Yang Z et al (2019a) Antimicrobial peptides with high proteolytic resistance for combating gram-negative bacteria. J Med Chem 62(5):2286–2304. https://doi.org/10.1021/acs.jmedchem.8b01348
24. Wang M, Lin J, Sun Q, Zheng K, Ma Y, Wang J (2019b) Design, expression, and characterization of a novel cecropin A-derived peptide with high antibacterial activity. Appl Microbiol Biotechnol 103:1765–1775. https://doi.org/10.1007/s00253-018-09592-z
25. Yang H, Wang L, Yuan L, Du H, Pan B, Lu K (2022) Antimicrobial Peptides with Rigid Linkers against Gram-Negative Bacteria by Targeting Lipopolysaccharide. J Agric Food Chem 70(50):15903–15916. https://doi.org/10.1021/acs.jafc.2c05921
26. Yang L, Sun Y, Xu Y et al (2020) Antibacterial peptide BSN-37 kills extra-and intra-cellular salmonella enterica serovar typhimurium by a nonlytic mode of action. Front Microbiol 11:174. https://doi.org/10.3389/fmicb.2020.00174
27. Zhang R, Fan X, Jiang X, Zou M, Xiao H, Wu G (2020) Multiple mechanisms of the synthesized antimicrobial peptide TS against Gram-negative bacteria for high efficacy antibacterial action in vivo. Molecules 26(1):60. https://doi.org/10.3390/molecules26010060
28. Zhao D, Ma L, Lu K, Wu J, He J (2015) Syntheses of valpromide dipeptide derivatives and interactions of derivatives with ctDNA. Res Chem Intermed 41:8591–8601. https://doi.org/10.1007/s11164-014-1913-1
29. Zhong G, Cheng J, Liang ZC et al (2017) Short synthetic β-sheet antimicrobial peptides for the treatment of multidrug-resistant pseudomonas aeruginosa burn wound infections. Adv Healthc Mater 6(7):1601134. https://doi.org/10.1002/adhm.201601134
30. Zhou X, Zhang G, Pan J (2015) Groove binding interaction between daphnetin and calf thymus DNA. Int J Biol Macromol 74:185–194. https://doi.org/10.1016/j.ijbiomac.2014.12.018

Figures

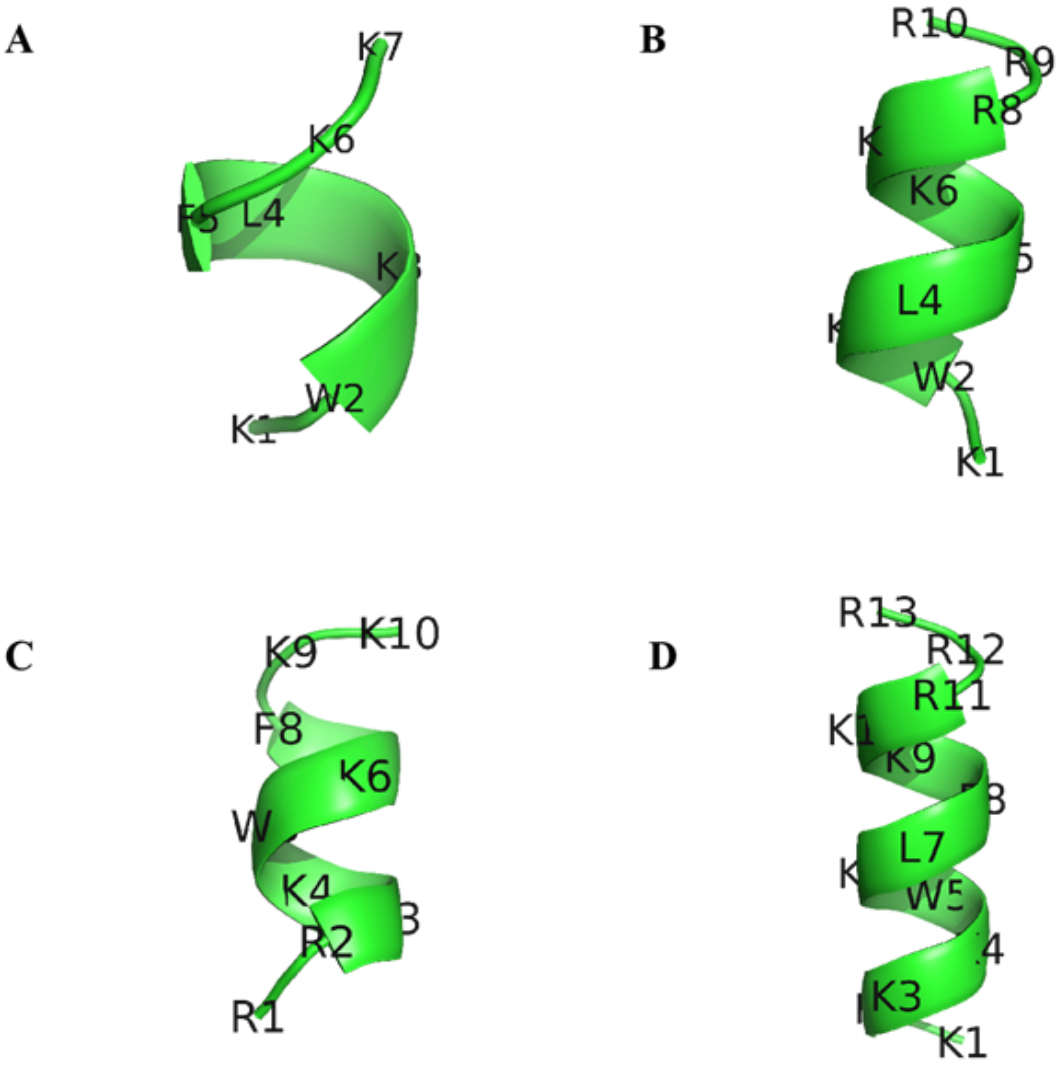

Figure 1

Predicted three-dimensional structures of CA (A), CA2 (B), CA3 (C), and CA4 (D)

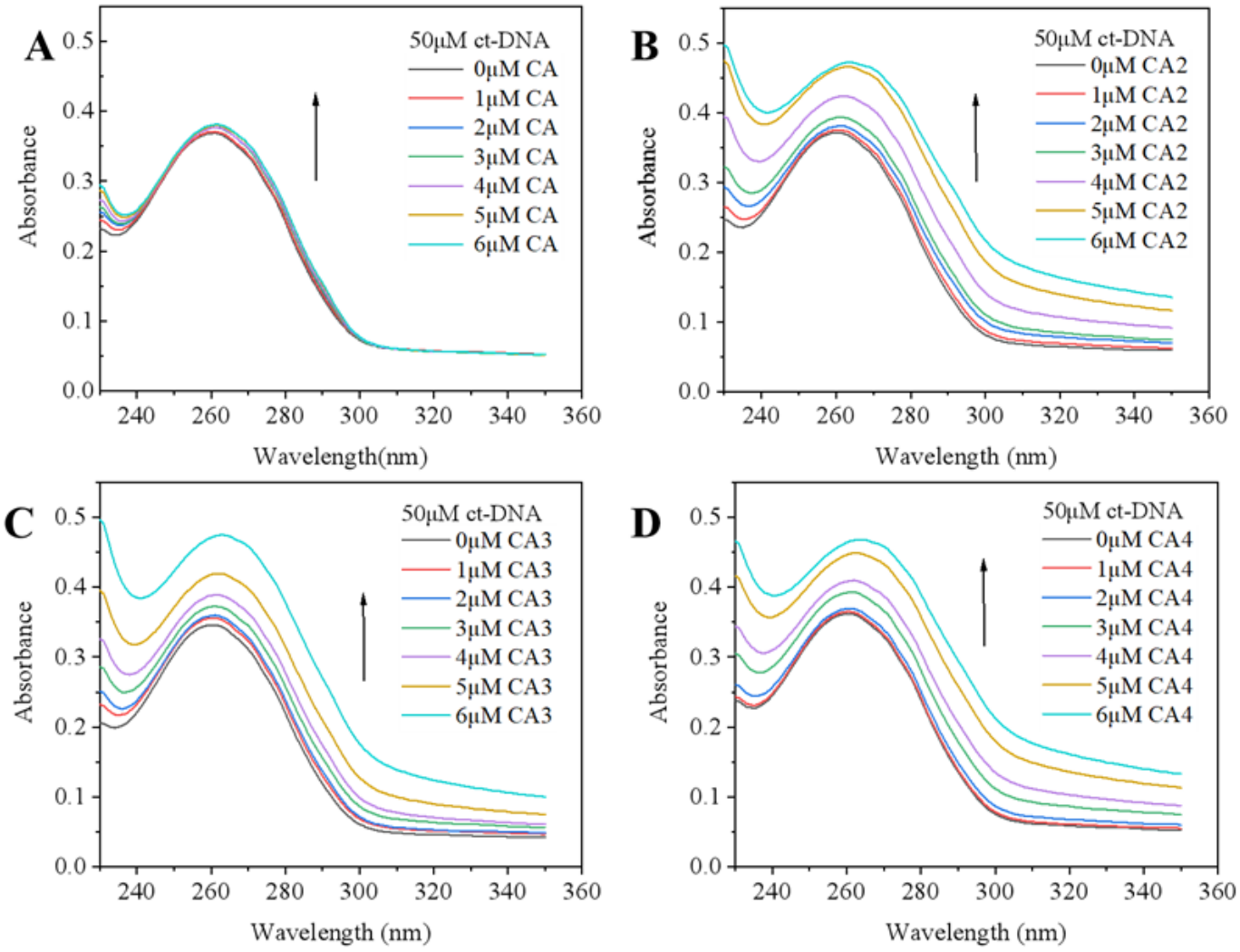

Figure 2

UV spectra of ct-DNA (Cct-DNA=50 μM) after addition of peptide solution. CA(A), CA2 (B), CA3 (C), and CA4 (D).

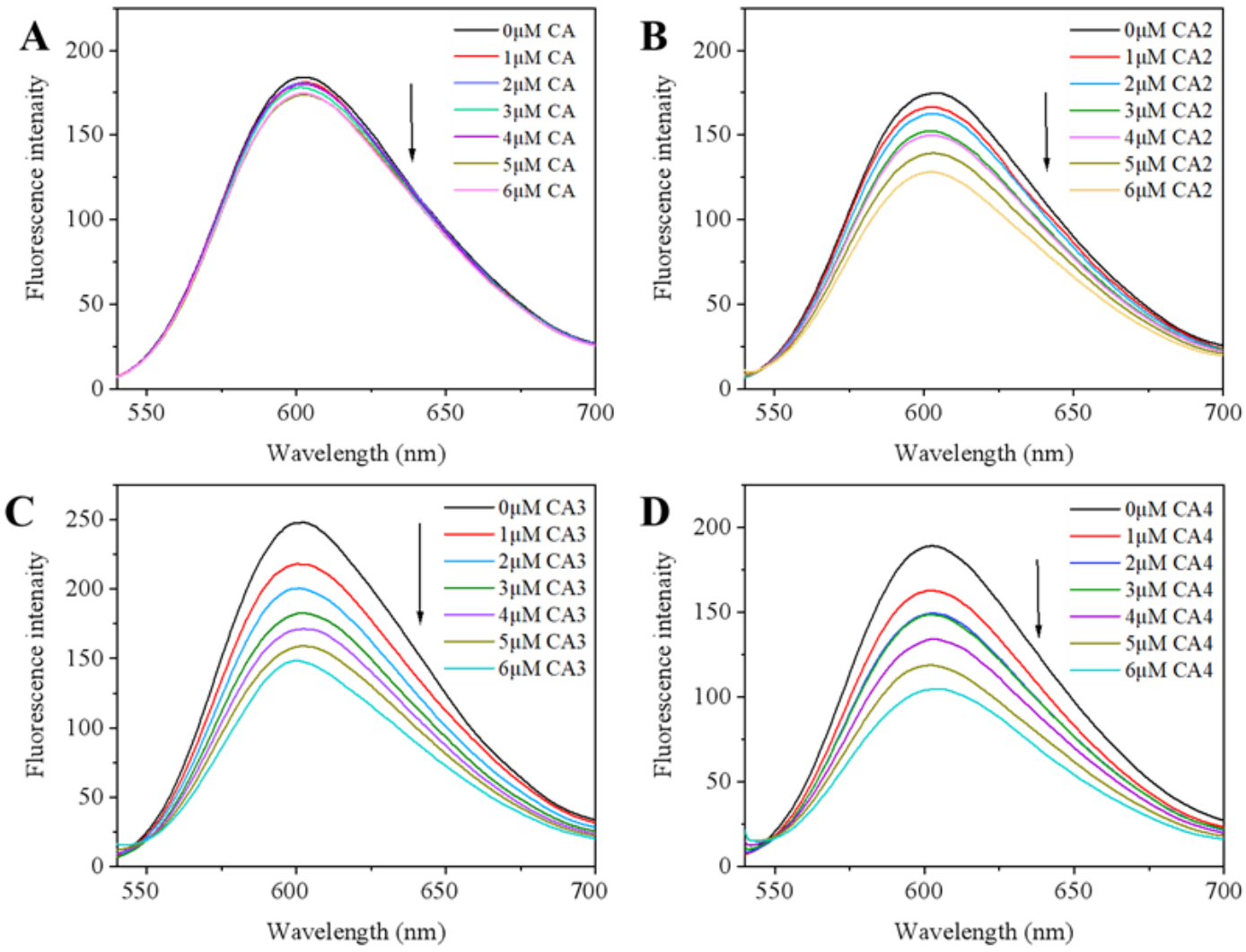

Figure 3

Fluorescence spectra of the DNA-EB system($C_{ct\text{-}DNA}$=50 μM, C_{EB}=5 μM) after addition of the peptide solution. CA (A), CA2 (B), CA3 (C), and CA4 (D).

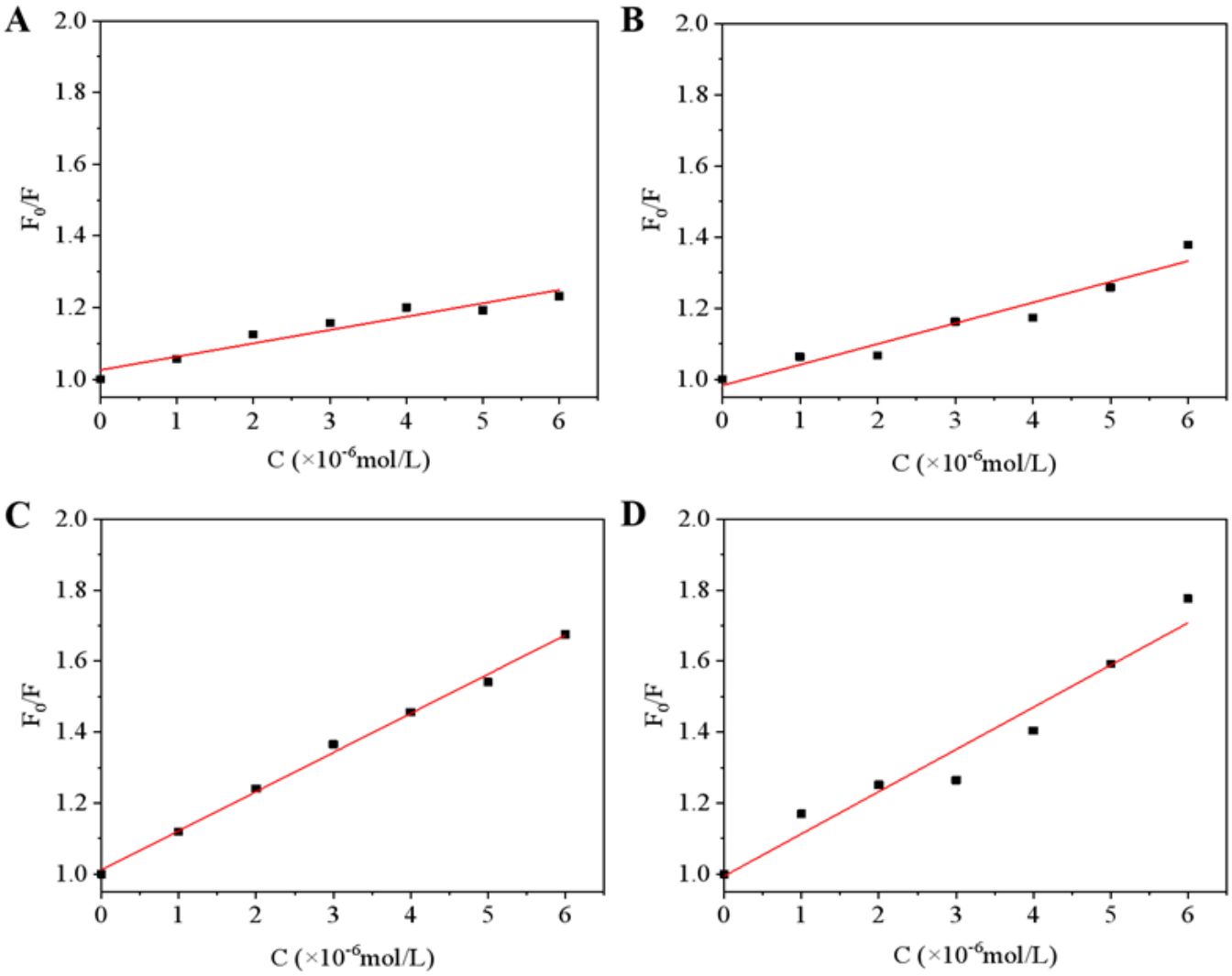

Figure 4

Stern-Volmer plots of the DNA-EB system ($C_{ct\text{-}DNA}$=50 μM, C_{EB}=5 μM) after addition of peptide solutions. CA (A), CA2 (B), CA3 (C), and CA4 (D).

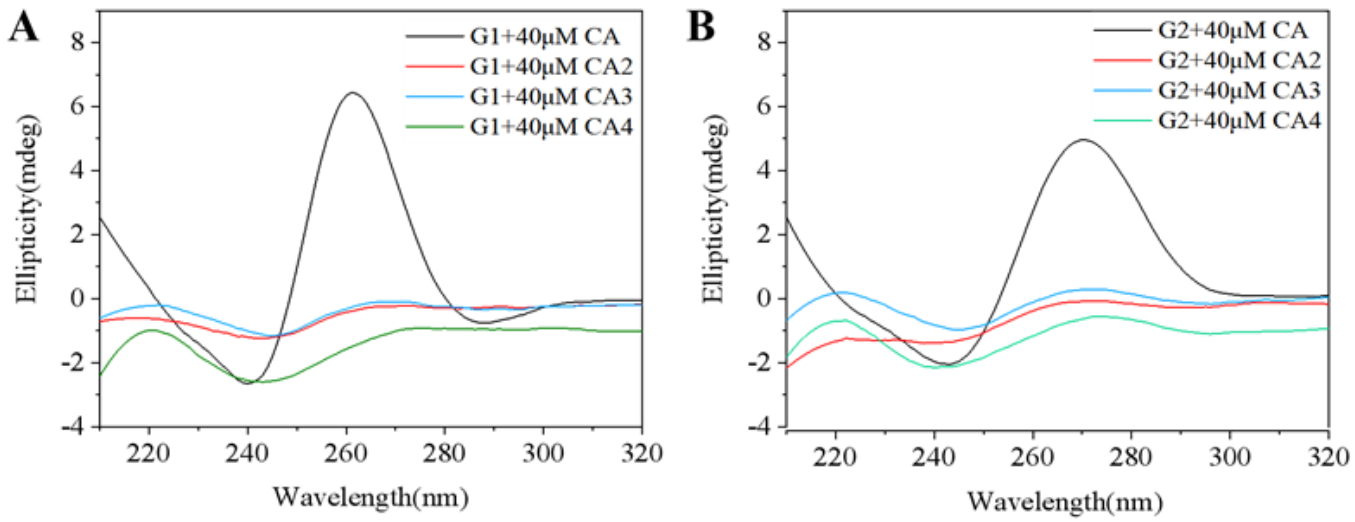

Figure 5

CD spectra of CA, CA2, CA3, and CA4 bound to G1(A) and G2(B).

Supplementary Files

This is a list of supplementary files associated with this preprint. Click to download.

- GraphicalAbstract.jpg
- Supplementarymaterials.doc